Geomechanics and Engineering, *Vol. 40, No. 6 (2025) 459-467*
https://doi.org/10.12989/gae.2025.40.6.459

Exploring AI-driven computational dynamic modeling and nanomechanical reinforcement for enhanced nonlinear post-buckling in plates: A comprehensive computer analysis

Pingquan Wang[1], Bo Zhang*[2], H. Karemt[3] and P. Politad[4]

[1]*Yangzhou Polytechnic Institute, Yangzhou 225127, Jiangsu, China*
[2]*School of Computer Science, Wuhan Donghu College, Wuhan 430212, Hubei, China*
[3]*Advanced Research and Development Center, LIPS Research Foundation, European International University, Paris, France*
[4]*Department of Computer Enngineering, University of Zabol, Zabol, Iran*

(*Received September 14, 2024, Revised February 3, 2025, Accepted March 9, 2025*)

Abstract. AI driven computational dynamic modeling and nanomechanical reinforcement of functionally graded (FG) plates resting on polymeric foundation are considered in the study and improvements of nonlinear post buckling behavior are assessed. Nonlinear characteristics are significantly improved by a proper exploitation of the superior mechanical properties of carbon nanotubes (CNTs). This analysis is enabled by a modified mixture homogenization approach coupled with a high order shear deformation theory (HSDT), which is useful in analyzing the distribution of nanocomposite property across the plate thickness. In the present research, key parameters such as CNT volume fraction, foundation stiffness, nanoparticle agglomeration, and dynamic loading intensity are studied comprehensively under nonlinear interactions to evaluate the bearing ability of system stability and dynamic response. In order to capture the complete nonlinear postbuckling and dynamic behavior, an advanced computational framework unites AI driven modeling with both energy principles and domain decomposition, Rayleigh-Ritz methods, and Newton Raphson numerical iteration. The results indicate that CNT reinforcement improves load bearing capacity and structural stability and polymeric composition has a pronounced effect on nonlinear dynamic properties in the form of damping and stability performance. For the front engineering of FG nanocomposite structures that enhance their mechanical resilience, this research is yielding critical learning on computational strategies for encouraging AI assisted material design and structural optimization.

Keywords: AI-driven computational; nanoparticles; newton-raphson technique; nonlinear behavior; plate

1. Introduction

The analysis and design of complex engineering structures particularly its continua have been significantly changed by advances in artificial intelligence (AI) and computational mechanics. The functionally graded (FG) plates reinforced with nanomaterials is an area of growing interest in terms of nonlinear post buckling behavior. Mechanically, these structures are endowed with an advantage of enhanced mechanical performance, stability, and durability in extreme loading conditions, and are frequently applied in aerospace, automotive, and civil engineering field (Liu *et al.* 2025, Yao *et al.* 2024, Zhao *et al.* 2025a, Zhou *et al.* 2017, Zhou *et al.* 2018).

Several modern approaches exist for modeling various structures among new theoretical models. New theories implemented by Tounsi and co-authors consist of Bessaim *et al.* (2013), Attia *et al.* (2024), Özkılıç *et al.* (2021), Amezcua and Ayala (2023). The classical plate theory (CLPT) employs Kirchhoff's hypothesis to establish that normal mid-plane straight lines will remain straight and perpendicular to the mid-plane under all conditions of thickness stretching. An application of CLPT is restricted to thin plates because it neglects transverse shear deformation effects during which thick plates require a different approach. The FSDT functions better than the CLPT since transverse shear deformation receives consideration through this model. The transverse shear strain of this theory remains uniform throughout the thickness layer which requires implementation of shear correction factors for proper strain energy calculation. Al-Basyouni *et al.* (2015) investigated FG beam size dependent bending together with vibration analysis using modified couple stress theory at neutral surface position (Zhao *et al.* 2025b, Peng *et al.* 2025, Wang *et al.* 2024a, Hu *et al.* 2024, Guo *et al.* 2024). Several studies have focused on examining the mechanical properties of plate during the previous years. Multiple engineers have published reports about nanostructure mechanical investigations (Belkorissat *et al.* 2024, Ahouel *et al.* 2023, Bellifa *et al.* 2017).

Modern material science achievements together with manufacturing reforms created new technologies including biomimetic 4D printing besides self-healing composites and functionally graded materials (FGMs) with superior mechanical characteristics (Wang *et al.* 2024b, Cong *et al.* 2024, Wang *et al.* 2025, Alam *et al.* 2025, Guo and Alam 2025). The scientific advances in materials engineering

*Corresponding author, Dr.
E-mail: zhangbo@wdu.edu.cn

ISSN: 2005-307X (Print), 2092-6219 (Online)

have introduced revolutionary solutions for aerospace technologies along with medical devices and structural frameworks. Research into biomimetic 4D printing has intensified markedly because this technique enables material-based time-responsive shape transformation of intelligent adaptive structures (Kanu *et al.* 2019a). Scientists have studied self-healing composites to understand their capability of repairing themselves autonomously which stretches the operational cycle of components under repetitive stress (Kanu *et al*. 2019b). Structural integrity demands respond through functionally graded materials because these systems optimize mechanical properties through gradual property adjustments along their composition profile. Multiple researchers have investigated the applications of these materials for fracture mechanics studies as well as vibration analysis and studying structural stability (Kanu *et al.* 2019c). Smart self-lubricating composites have exhibited successful outcomes in decreasing mechanical system wear and friction which improves operational performance according to Kanu *et al.* (2021a). Scientists have performed numerical assessments of prosthetic bone plates that treat pediatric bone fractures through finite element analysis showing its significant medical value (Kanu *et al*. 2020a). Scientific studies have demonstrated pediatric femur fracture bone plates with functional gradients which perform better under compressive and torsional loading circumstances (Kanu *et al.* 2021b). Researchers studied the nonlinear deflection qualities of nanoclay-enforced polymer hybrid composite plates containing carbon nanotubes and extra loading parameters (Lal and Kanu 2020b). Research streams concentrate on secondary deformation of ultrafine SiC particle-reinforced metal matrix composites intended for high-performance applications since these materials show superior mechanical properties (Kanu *et al*. 2021c). The reaction surface methodology (RSM) finds optimal 3D printing parameters for FDM which produces precise complex structures appropriate for industrial along with medical applications (Vates *et al*. 2021a). The modeling of stress waves in matrix cracked laminates has delivered important damage mechanics knowledge for composite materials (Kanu *et al.* 2021d). Inverse heat conduction algorithms assisted Pandey *et al.* (2021) to discover essential thermal features of AZ31-alloy and H13-die combinations which became a major development in heat transfer and energy efficiency research. Scientists have determined that carbon nanotubes show promise in water filtration operations because they efficiently remove contaminants (Jain and Kanu 2021). The investigation of sustainable engineering involves designing aluminum alloy-based vortex tubes with multiple inlet nozzles followed by their CFD analysis to optimize their performance across different industrial applications (Kanu *et al.* 2021e). Higher-order shear deformation theory forms the basis for recent research about CNT fiber-reinforced and nanoclay-modified polymer matrix hybrid composite plates when evaluating their post-buckling responses under in-plane buckling loads (Kanu and Lal 2022a). Studies on aluminum-based hybrid metal matrix composites have investigated their mechanical properties as well as tribological behaviors to develop advanced materials which excel at resisting wear (Gonfa 2 *et al.* 2022b). Research conducted by experts from multiple fields has led to progress in materials science together with structural engineering and biomedical applications which develops advanced adaptive structures alongside smart materials for future use.

This work looks into the integration of AI driven computational dynamic modeling with nanomechanical reinforcement for enhancing nonlinear post buckling response of plates. The use of carbon nanotubes (CNTs) as nanomechanical reinforcements demonstrates great potential to improve FG plate structural behavior. Carbon nanotubes possess extraordinary mechanical quality which enhance load-bearing capacity and damping characteristics and stability levels of structures. Highly precise modeling of material properties interactions with structural behavior and external force dynamics needs advanced computational approaches to yield accurate results. The study utilizes advanced AI-enhanced modeling methods combined with HSDT theory and energy principles as well as Rayleigh-Ritz method and Newton-Raphson iteration numerical methods. The combination of these analytical methods provides complete evaluation of key factors associated with CNT volume distribution and nanoparticle cluster behavior as well as polymeric foundation elasticity and dynamic force magnitudes. AI-driven computational strategies enable this research to explore enhanced understanding of nanocomposite FG plate behavior both during and after buckling phenomena. The research findings enable progress in developing high-performance resistant materials which inspire advanced engineering design of structural components.

2. Formulation

As shown on the Fig. 1, a plate on a foundation is presented. The plate is found to be smooth and flat and the polymeric foundation that supports the plate provides structural support. The illustration shows clearly the interaction of the plate with its polymeric base, which may be useful in how to consider the mechanical stability, reinforce the material, or distribute load for composite structures. The length, width and thickness of plate are shown with length a, width b and thickness h.

Mindlin theory which is the extension of classical plate theory that incorporates the effects of transverse shear deformation and rotary inertia in order to increase the accuracy in describing of thick plates. Mindlin theory, unlike Kirchhoff plate theory that postulates normal sections to continue to be normal to the mid surface in the deformed configuration, takes into consideration shear flexibility and thus provides more accurate predictions on the deflections and stresses in moderately thick and thick plates. Three governing equations for displacement components and rotation angles are derived in this theory and they define more comprehensive analysis of bending, vibration and buckling behaviour of plates. Most of

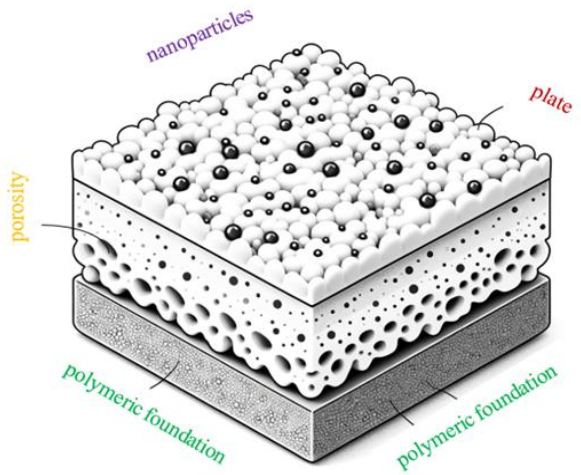

Fig. 1 A schematic of a plate with CNT surrounded with polymeric foundation

all, Mindlin's formulation is very useful in engineering applications involving composite sandwiches and functionally graded materials, where shear effects are significant (Reddy and Wang 2020):

The deflection field for this figure is

$$u(x,y,z)=u(x,y)+z\phi_x(x,y), \tag{1}$$

$$v(x,y,z)=v(x,y)+z\phi_y(x,y), \tag{2}$$

$$w(x,y,z)=w(x,y), \tag{3}$$

where u, v and w are in-plane displacements and ϕ_x and ϕ_y are the. The strain relations are:

$$\begin{Bmatrix}\varepsilon_{xx}\\ \varepsilon_{yy}\\ \gamma_{yz}\\ \gamma_{xz}\\ \gamma_{xy}\end{Bmatrix}=\begin{Bmatrix}\varepsilon^0_{xx}\\ \varepsilon^0_{yy}\\ \gamma^0_{yz}\\ \gamma^0_{xz}\\ \gamma^0_{xy}\end{Bmatrix}+z\begin{Bmatrix}\varepsilon^1_{xx}\\ \varepsilon^1_{yy}\\ \gamma^1_{yz}\\ \gamma^1_{xz}\\ \gamma^1_{xy}\end{Bmatrix}, \tag{4}$$

where

$$\begin{Bmatrix}\varepsilon^0_{xx}\\ \varepsilon^0_{yy}\\ \gamma^0_{yz}\\ \gamma^0_{xz}\\ \gamma^0_{xy}\end{Bmatrix}=\begin{Bmatrix}\frac{\partial u}{\partial x}+\frac{1}{2}\left(\frac{\partial w}{\partial x}\right)^2\\ \frac{\partial v}{\partial y}+\frac{1}{2}\left(\frac{\partial w}{\partial y}\right)^2\\ \frac{\partial w}{\partial y}+\phi_y\\ \frac{\partial w}{\partial x}+\phi_x\\ \frac{\partial u}{\partial y}+\frac{\partial v}{\partial x}+\frac{\partial w}{\partial x}\frac{\partial w}{\partial y}\end{Bmatrix}, \tag{5}$$

$$\begin{Bmatrix}\varepsilon^1_{xx}\\ \varepsilon^1_{yy}\\ \gamma^1_{yz}\\ \gamma^1_{xz}\\ \gamma^1_{xy}\end{Bmatrix}=\begin{Bmatrix}\frac{\partial \phi_x}{\partial x}\\ \frac{\partial \phi_y}{\partial y}\\ 0\\ 0\\ \frac{\partial \phi_x}{\partial x}+\frac{\partial \phi_y}{\partial y}\end{Bmatrix}. \tag{6}$$

3. Extended rule of mixture

This study has a composite plate which is polymer matrix reinforced with CNTs. The models are for four different types of layup through the thickness of CNT: FG-UD, FG-X, FG-A, and FG-O. The rule of mixtures is applied to determine the mechanical properties of this composite structure (Singh and Prakash 2018)

$$E_{11}=\eta_1 V_{CNT}E_{11}^{CNT}+V_m E^m, \tag{7}$$

$$\frac{\eta_2}{E_{22}}=\frac{V_{CNT}}{E_{22}^{CNT}}+\frac{V_m}{E^m}, \tag{8}$$

$$\frac{\eta_3}{G_{12}}=\frac{V_{CNT}}{G_{12}^{CNT}}+\frac{V_m}{G^m}, \tag{9}$$

$$V_{CNT}+V_m=1. \tag{10}$$

where E is Young's moduli and G is shear modulus; super index m and CNT are for polymer plate and CNTs, respectively. Also, V_{CNT} and V_m are volume fractions of CNT and polymer plate, respectively which are for various distributions as

$$V_{CNT}=V^*_{CNT}, \qquad (UD) \tag{11}$$

$$V_{CNT}=\left(1-\frac{2z}{h}\right)V^*_{CNT}, \qquad (FG-A) \tag{12}$$

$$V_{CNT}=2\left(1-\frac{2|z|}{h}\right)V^*_{CNT}, \qquad (FG-O) \tag{13}$$

$$V_{CNT}=2\left(\frac{2|z|}{h}\right)V^*_{CNT}, \qquad (FG-X) \tag{14}$$

where

$$V^*_{CNT}=\frac{W_{CNT}}{W_{CNT}+\left(\frac{\rho_{CNT}}{\rho_m}\right)-\left(\frac{\rho_{CNT}}{\rho_m}\right)W_{CNT}}, \tag{15}$$

where w_{CNT} is the mass fraction of CNTs, ρ_{CNT} and ρ_m are the densities of CNTs and polymer matrix, respectively. The

Poisson's ratio is:

$$\upsilon_{12} = V_{CNT}\upsilon_{12}^{CNT} + V_m\upsilon^m, \tag{16}$$

$$\rho = V_{CNT}\rho^{CNT} + V_m\rho^m, \tag{17}$$

where υ_{12}^{CNT} and υ^m are Poisson's ratios of CNT and polymer matrix, respectively.

4. Energy method

The strain energy of the plate is

$$U = \frac{1}{2}\int_A \int_{\frac{-h}{2}}^{\frac{h}{2}} \left(\sigma_{xx}\varepsilon_{xx} + \sigma_{yy}\varepsilon_{yy} + \sigma_{yz}\gamma_{yz} + \sigma_{xz}\gamma_{xz} + \sigma_{xy}\gamma_{xy}\right) dz dA. \tag{18}$$

where the stress relations are

$$\begin{Bmatrix} \sigma_{xx} \\ \sigma_{yy} \\ \sigma_{yz} \\ \sigma_{xz} \\ \sigma_{xy} \end{Bmatrix} = (1-e_0) \begin{bmatrix} Q_{11} & Q_{12} & 0 & 0 & 0 \\ & Q_{22} & 0 & 0 & 0 \\ & & Q_{44} & 0 & 0 \\ & & & Q_{55} & 0 \\ sym. & & & & Q_{66} \end{bmatrix} \begin{Bmatrix} \varepsilon_{xx} \\ \varepsilon_{yy} \\ \gamma_{yz} \\ \gamma_{xz} \\ \gamma_{xy} \end{Bmatrix}, \tag{19}$$

where e_0 is porosity parameter. With define of below relations

$$\begin{Bmatrix} N_{xx} \\ N_{yy} \\ N_{xy} \end{Bmatrix} = \int_{\frac{-h}{2}}^{\frac{h}{2}} \begin{Bmatrix} \sigma_{xx} \\ \sigma_{yy} \\ \sigma_{xy} \end{Bmatrix} dz, \tag{20}$$

$$\begin{Bmatrix} M_{xx} \\ M \\ M_{xy} \end{Bmatrix} = \int_{\frac{-h}{2}}^{\frac{h}{2}} z \begin{Bmatrix} \sigma_{xx} \\ \sigma_{yy} \\ \sigma_{xy} \end{Bmatrix} dz, \tag{21}$$

$$\begin{Bmatrix} Q_y \\ Q_x \end{Bmatrix} = \kappa_s \int_{\frac{-h}{2}}^{\frac{h}{2}} \begin{Bmatrix} \sigma_{yz} \\ \sigma_{xz} \end{Bmatrix} dz, \tag{22}$$

where k_s is the shear correction coefficient, we have

$$\begin{aligned} U = \frac{1}{2}\int_A \Bigg(& N_{xx}\left(\frac{\partial u}{\partial x} + 0.5\left(\frac{\partial w}{\partial x}\right)^2\right) + M_{yy}\frac{\partial \phi_y}{\partial y} \\ & + N_{yy}\left(\frac{\partial v}{\partial y} + 0.5\left(\frac{\partial w}{\partial y}\right)^2\right) + M_{xx}\frac{\partial \phi_x}{\partial x} \\ & + N_{xy}\left(\frac{\partial u}{\partial y} + \frac{\partial v}{\partial x} + \left(\frac{\partial w}{\partial x}\right)\left(\frac{\partial w}{\partial y}\right)\right) + Q_x\left(\frac{\partial w}{\partial x} + \phi_x\right) \\ & + M_{xy}\left(\frac{\partial \phi_x}{\partial y} + \frac{\partial \phi_y}{\partial x}\right) + Q_y\left(\frac{\partial w}{\partial y} + \phi_y\right)\Bigg) dA. \end{aligned} \tag{23}$$

With the help of Eqs. (4)-(6) and Eq. (19), we have

$$\begin{aligned} N_{xx} = {} & A_{11}\frac{\partial u}{\partial x} + B_{11}\frac{\partial \phi_x}{\partial x} + \frac{1}{2}A_{11}\left(\frac{\partial w}{\partial x}\right)^2 \\ & + A_{12}\frac{\partial v}{\partial y} + B_{12}\frac{\partial \phi_y}{\partial y} + \frac{1}{2}A_{12}\left(\frac{\partial w}{\partial y}\right)^2, \end{aligned} \tag{24}$$

$$\begin{aligned} N_{yy} = {} & A_{12}\frac{\partial u}{\partial x} + B_{12}\frac{\partial \phi_x}{\partial x} + \frac{1}{2}A_{12}\left(\frac{\partial w}{\partial x}\right)^2 \\ & + A_{22}\frac{\partial v}{\partial y} + B_{22}\frac{\partial \phi_y}{\partial y} + \frac{1}{2}A_{22}\left(\frac{\partial w}{\partial y}\right)^2, \end{aligned} \tag{25}$$

$$\begin{aligned} N_{xy} = {} & A_{66}\frac{\partial v}{\partial x} + B_{66}\frac{\partial \phi_y}{\partial x} + A_{66}\frac{\partial u}{\partial y} \\ & + B_{66}\frac{\partial \phi_x}{\partial y} + A_{66}\left(\frac{\partial w}{\partial x}\right)\left(\frac{\partial w}{\partial y}\right), \end{aligned} \tag{26}$$

$$\begin{aligned} M_{xx} = {} & B_{11}\frac{\partial u}{\partial x} + D_{11}\frac{\partial \phi_x}{\partial x} + 0.5\,B_{11}\left(\frac{\partial w}{\partial x}\right)^2 \\ & + B_{12}\frac{\partial v}{\partial y} + D_{12}\frac{\partial \phi_y}{\partial y} + 0.5\,B_{12}\left(\frac{\partial w}{\partial y}\right)^2, \end{aligned} \tag{27}$$

$$\begin{aligned} M_{yy} = {} & B_{12}\frac{\partial u}{\partial x} + D_{12}\frac{\partial \phi_x}{\partial x} + 0.5\,B_{12}\left(\frac{\partial w}{\partial x}\right)^2 \\ & + B_{22}\frac{\partial v}{\partial y} + D_{22}\frac{\partial \phi_y}{\partial y} + 0.5\,B_{22}\left(\frac{\partial}{\partial y}w\right)^2, \end{aligned} \tag{28}$$

$$\begin{aligned} M_{xy} = {} & B_{66}\frac{\partial v}{\partial x} + D_{66}\frac{\partial \phi_y}{\partial x} + B_{66}\frac{\partial u}{\partial y} \\ & + D_{66}\frac{\partial \phi_x}{\partial y} + B_{66}\left(\frac{\partial w}{\partial x}\right)\left(\frac{\partial w}{\partial y}\right), \end{aligned} \tag{29}$$

$$Q_{xz} = \kappa_s A_{55}\frac{\partial w}{\partial x} + \kappa_s A_{55}\phi_x, \tag{30}$$

$$Q_{yz} = \kappa_s A_{44}\frac{\partial w}{\partial y} + \kappa_s A_{44}\phi_y. \tag{31}$$

where

$$\left(A_{ij}, B_{ij}, D_{ij}\right) = \int_{\frac{-h}{2}}^{\frac{h}{2}} Q_{ij}(z)\left(1, z, z^2\right) dz. \tag{32}$$

The plate is surrounded by polymeric medium which its work is

$$W_f = -\int_A \left(K_w w - G_p \nabla^2 w\right) w\, dA, \tag{33}$$

K_w and G_p are spring and shear parameters, respectively.

Finally, the total energy is

$$\begin{aligned}\Pi = U - W = \int_A \left\{ \frac{1}{2}\left[\right. \right. & xx\left(\frac{\partial u}{\partial x}+0.5\left(\frac{\partial w}{\partial x}\right)^2\right) \\ & + N_{yy}\left(\frac{\partial v}{\partial y}+0.5\left(\frac{\partial w}{\partial y}\right)^2\right)+N_{xy}\left(\frac{\partial u}{\partial y}+\frac{\partial v}{\partial x}+\left(\frac{\partial w}{\partial x}\right)\left(\frac{\partial w}{\partial y}\right)\right) \\ & + M_{xx}\frac{\partial \phi_x}{\partial x}+M_{yy}\frac{\partial \phi_y}{\partial y}+M_{xy}\left(\frac{\partial \phi_x}{\partial y}+\frac{\partial \phi_y}{\partial x}\right) \\ & \left. + Q_x\left(\frac{\partial w}{\partial x}+\phi_x\right)+Q_y\left(\frac{\partial w}{\partial y}+\phi_y\right)\right] \\ & \left. + \left[\left(K_w w - G_p \nabla^2 w\right) w\right]\right\} dA. \end{aligned} \tag{34}$$

5. Nonlinear analysis

The displacements based on the simply supported boundary conditions are

$$w(x,y) = w_{mn}\, sin\left(\frac{m\pi x}{a}\right) sin\left(\frac{n\pi y}{b}\right), \tag{35}$$

$$\phi_x(x,y) = \phi_{xmn}\, cos\left(\frac{m\pi x}{a}\right) sin\left(\frac{n\pi y}{b}\right), \tag{36}$$

$$\phi_y(x,y) = \phi_{ymn}\, sin\left(\frac{m\pi x}{a}\right) cos\left(\frac{n\pi y}{b}\right), \tag{37}$$

where m and n are mode numbers. By using Eqs. (35-37), we have:

$$\left(K_L + K_{NL} - Force K_G\right) Y = 0, \tag{38}$$

where K_L, K_{NL} and K_G are linear, nonlinear and geometric matrices, respectively. By using the Rayleigh-Ritz method, the nonlinear response can be obtained.

The Rayleigh-Ritz method serves as a popular approximation tool for structural mechanics and applied mathematics to find solutions for eigenvalue problems during stability and vibration studies. The method relies on minimizing system total potential energy through appropriate choice of trial functions which meet boundary condition requirements. The method makes use of trial functions that express unknown coefficients between admissible shape functions. The substitution of displacement assumptions alongside variational principle analysis allows the method to simplify the problem through algebraic systems which yield approximate natural frequencies or critical loads. The accuracy of Rayleigh-Ritz method depends on which trial functions users select alongside their number because this simplifies the analysis of complex mechanical systems.

6. Numerical results

The assessment of FG plates supported by a polymeric foundation investigates how advanced nano-mechanics modifications and nanoparticle reinforcement affects their nonlinear behavior in this section. The numerical analysis uses a HSDT for obtaining results focused on modeling the complex mechanical response of structural components. The study investigates the impact of multiple variables starting from nanoparticle volume fraction followed by grading index and ending with foundation stiffness and loading parameters on plate deflection response and stress distributions and stability behavior. The material properties of CNTs and polyurethane foam plate are listed in Table 1.

Table 1 The material properties of CNTs and polyurethane plate

polyurethane	CNTs
$E^m = 6MPa$	$E_{11}^{CNT} = 5.6466(TPa)$
$\upsilon_m = 0.34$	$E_{22}^{CNT} = 7.08(TPa)$
	$G_{12}^{CNT} = 1.9447(TPa)$
	$\upsilon_{12}^{CNT} = 0.175$

Fig. 2 provides visual evidence of how aspect ratio affects the dimensionless post-buckling load which can be measured through dimensionless deflection amplitude values. A substantial modification in the post-buckling response occurs in FG polyurethane foam-based plates when aspect ratio values change. An increase in the aspect ratio results in both a reduction of post-buckling load levels and structural stiffness parameters. Larger aspect ratio plates become more flexible during deflection because of their slender nature which makes them prone to geometric nonlinearities. The structural rigidity of the plates increases when their aspect ratios decrease which leads to better resistance against post-buckling deformations.

The post-buckling response sensitivity to aspect ratio increases exponentially as deflection amplitude increases according to Fig. 2.

The research investigates how polymeric elastic medium influences polyurethane plates which rest upon polymeric foundations after buckling occurs. The post-buckling behavior strongly depends on both the dimensionless Winkler modulus parameter and the shear modulus parameter as shown in Figs. 3 and 4. The compressive

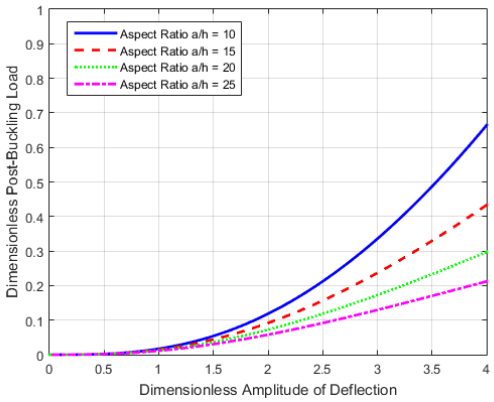

Fig. 2 The impact of aspect ratio on the dimensionless post-buckling load as a function of dimensionless deflection

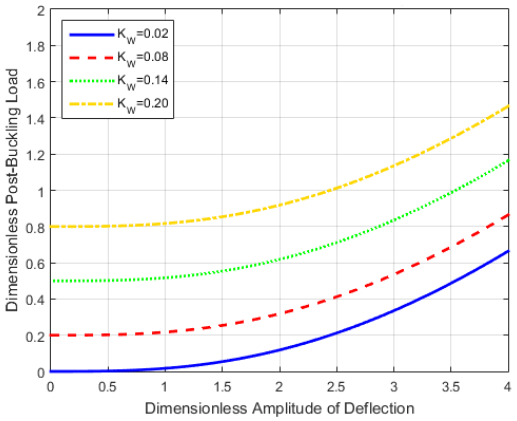

Fig. 3 The impact of spring constant of polymeric foundation on the dimensionless post-buckling load as a function of dimensionless deflection

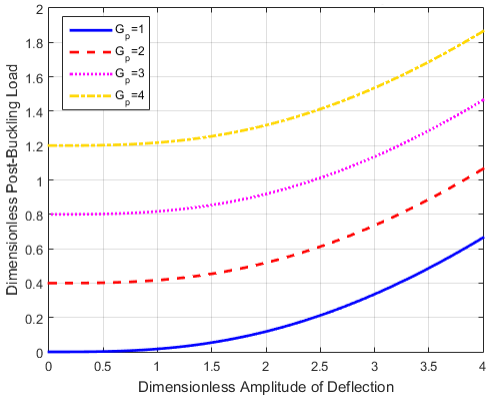

Fig. 4 The impact of shear constant of polymeric foundation on the dimensionless post-buckling load as a function of dimensionless deflection

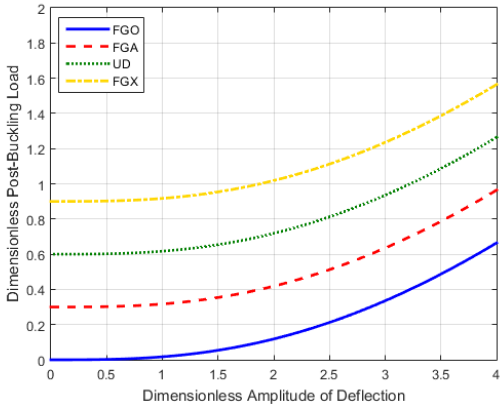

Fig. 5 The impact of CNTs distributions on the dimensionless post-buckling load as a function of dimensionless deflection

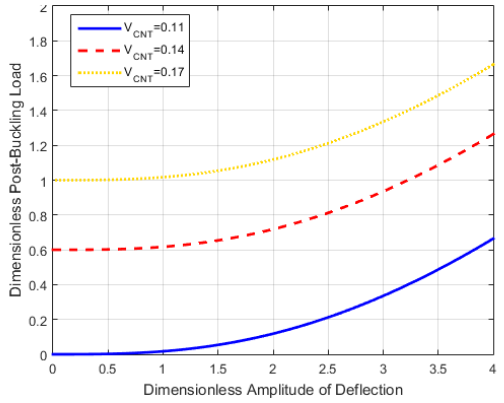

Fig. 6 The impact of CNTs percent on the dimensionless post-buckling load as a function of dimensionless deflection

stiffness of the elastic foundation is estimated by the Winkler modulus whereas the shear modulus determines the transverse shear interaction between the plate and support. The system stiffness improves when these parameters become larger thus generating stronger resistance against post-buckling deformations. The foundation generates additional reactive forces that fight against external loads to provide structure stability and boost its load capacity.
Plates supported on strong foundations delay their buckling response and produce higher subsequent load capacity than plates supported on weak foundations.

The post-buckling performance of polyurethane plates rises through the collaborative influence of both Winkler stiffness and shear modulus parameters as they control normal and shear interaction responses. A rise in Winkler modulus creates out-of-plane displacement constraint and boosts the lateral coupling effects from increased shearing modulus which reduces overall deflection amplitudes and avoids nonlinear instabilities. Merged foundation behavior stabilizes the load-deflection response after deformation which benefits structural systems needing compressive strength enhancement. Optimizing foundation properties stands as an effective method to boost functional polyurethane foam plate mechanical properties allowing their deployment for sophisticated nano-reinforced engineering systems.

Four different carbon nanotube (CNT)-based functionally graded distribution configurations demonstrate their impact on polyurethane plate post-buckling strength which can be observed in Fig. 5. Different post-buckling responses are observed depending on the FG distribution arrangement of CNTs. The distribution method which places carbon nanotubes outside the mid-plane results in maximum post-buckling strength among all tested configurations. The post-buckling resistance of the plate rises because distributing carbon nanotubes away from the neutral axis builds up its bending stiffness. Additional support from the polymeric foundation enhances plate stability under high loading conditions because the foundation combines with the bending stiffness enhancement of the polymeric bed. The mechanical performance of FG-CNTRC plates depends heavily on the distribution method of CNTs because it influences their structural behavior therefore proper optimization of spatial arrangements remains essential.

Furthermore, Fig. 6 investigates the effect of CNT volume fraction on the post-buckling response of the polyurethane plate. It is found that there is a significant

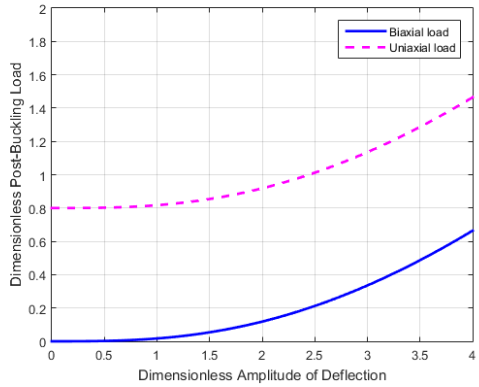

Fig. 7 The impact of load on the dimensionless post-buckling load as a function of dimensionless deflection

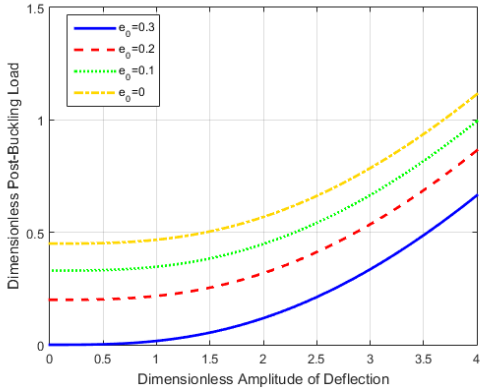

Fig. 8 The impact of porosity on the dimensionless post-buckling load as a function of dimensionless deflection

increase in post buckling load with the increase in the volume fraction of CNTs. This is expected as a higher volume fraction means higher number of CNTs present within the composite matrix and hence increase in stiffness, strength, and the ability to carry a load. The reinforcement of the plate increases resistance to large deflections in order of maintaining structural integrity at elevated post buckling loads. Moreover, the polymeric foundation complements this reinforcement by supporting better the stresses and the reduction of the localized deformations. These observations validate

The post buckling response of a polyurethane plate supported by a polymeric foundation according to deflection is shown in Fig. 7, considering biaxial and uniaxial loading. However, it is seen that the post-buckling load reduces drastically with biaxial compression compared to uniaxial loading. This is because application of compressive forces in the biaxial manner is highly intensified, due to which the load is multi intensified on the plate. Therefore, it takes the plate closer to being in its critical buckling state and consequently has less capability of sustaining greater post buckling loads. Additional stiffness is afforded by the polymeric foundation, but its contribution does not sufficiently balance out the way the instability is amplified by biaxial loading. Thus, under biaxial compression, post buckling strength of plate is reduced and deflections become larger than for the uniaxial sample.

In addition, the sensitivity to the way applied loads are applied is further shown through the difference in post-buckling response between biaxial and uniaxial loading conditions. Having a single dominant load direction in the uniaxial compression case gives the plate the greater stability which leads to a more gradual post-buckling progression. However, the biaxial loading results in the acceleration of the structural instability, resulting in the earlier failure or excessive deformation. In particular, this effect is highly important at finite strains and loads when mechanical properties and failure mechanisms of functionally graded polyurethane plates reinforced with CNTs depend on load distribution. The findings highlight the importance of paying close attention to the loading conditions in the design and utilization of polyurethane composite plates, to provide most structural performance for complex loading environments for engineering applications.

The effect of porosity on the dimensionless post-buckling load for polyurethane plates supported by a polymeric foundation is shown in Fig. 8, where making the figure dimensionless by dividing the top and bottom directions. The detrimental effect of porosity on the structural stability of the system is clear since it decreases the post-buckling load monotonically with increasing porosity. Porosity, introducing voids to the material thus reducing the materials overall density and stiffness, causes this to happen. Therefore, the bearing capacity of the plate is reduced, and the plate is more prone to deformation under compressive loads. Porosity increases the plate's flexibility, reducing the stiffness of the plate that makes it less resistant to post buckling deflections resulting in an earlier onset of a structural instability. However, it does buffer some of the loss of stiffness, but can do very little to offset the loss of stiffness with increasing porosity, which has such a negative effect at higher porosity levels.

Additionally, porosity is found to cause its effect more at elevated deflection amplitudes as the nonlinearities begin to dominate the monotonic and the post-buckling behavior. The mechanical performance of the plate is lost as the porosity level increases and greater deformation is being experienced for the same applied load. In the case of functionally graded polyurethane plates, where the pore distribution could be inhomogeneous, this effect is particularly important, as it may cause local weakening of a plate in certain areas.

In addition, a polymeric foundation is present that helps to stabilize the structure in some way, but its effectiveness lessens with increasing porosity. These results highlight the necessity of control over porosity in the manufacturing and design of polyurethane nanocomposite plates in order to maintain structural integrity and mechanical performance in the presence of post buckling resistance as a design criterion.

7. Conclusions

An AI-driven computational framework to analyze the nonlinear post-buckling behavior of functionally graded

(FG) plates strengthened with nanomechanical enhancements is generated in this study. The research integrates advanced AI based dynamic modeling with high order computational strategies to reveal deep insights of stability and mechanical performance of polyurethane foam based plates resting on polymeric foundations. The results highlight the important role of key parameters such as aspect ratio, foundation stiffness, CNT distribution, porosity, on post buckling response. It is shown that with increasing aspect ratio, stiffness and post buckling load carry capacity decrease, however polymeric foundations provide reactive force that increases stability particularly when winker modulus and shear modulus are larger. Moreover, the study underlines the importance of the placement and volume fraction of CNT for the reinforcement of structural performance. However, post buckling capacity is significantly improved by having CNTs located further from the midplane, and even greater loads can be carried and highly reduced excessive deflections with increased CNT concentration. Finally, it is shown that biaxial compression significantly reduces post buckling strength relative to uniaxial loading as the compressive forces tend to push the structure closer to instability. Although polymeric foundations provide stronger stiffness than the biaxial loaded structures, they cannot sufficiently recover the instability. Additionally, it is found that generally post buckling performance is degraded with increased porosity due to the decrease where the material stiffness and load bearing capacity is decreased and therefore the plates are more prone to excessive deformations. Nevertheless, the control over porosity distribution is still critical for the proper optimal mechanical behavior of polymeric foundations combined with CNT reinforcement. In this research, the AI driven modeling approach allows for more accurate predictions of nonlinear dynamic behavior of high performance nanocomposite plates with critical insights into plate design and optimization. They made these finding contribute to the development of intelligent computational strategies for enhancing the structural resilience of FG materials in critical engineering applications.

References

Ahouel, M., Houari, M.S.A., Adda Bedia, E.A. and Tounsi, A. (2023), "Size-dependent mechanical behavior of functionally graded trigonometric shear deformable nanobeams including neutral surface position concept", *Adv. Nano Res.*, **20**(5), 963-981. https://doi.org/10.12989/anr.2023.20.5.963.

Alam, M., Guo, Y., Bai, Y. and Luo, S. (2025), "Post-critical nonlinear vibration of nonlocal strain gradient beam involving surface energy effects", *J. Sound Vib.*, **601**, 118930. https://doi.org/10.1016/j.jsv.2025.118930.

Amezcua, H.R. and Ayala, A.G. (2023), "A computationally efficient numerical integration scheme for non-linear planestress/strain FEM applications using one-point constitutive model evaluation", *Struct. Eng. Mech.*, **85**(1), 89-104. https://doi.org/10.12989/sem.2023.85.1.089.

Al-Basyouni, K.S., Tounsi, A. and Mahmoud, S.R. (2015), "Size dependent bending and vibration analysis of functionally graded beams based on modified couple stress theory and neutral surface position", *Compos. Struct.*, **125**, 621-630, https://doi.org/10.1016/j.compstruct.2015.02.048.

Attia, A., Tounsi, A., Adda Bedia, E.A. and Mahmoud, S.R. (2024), "Free vibration analysis of functionally graded plates with temperature-dependent properties using various four variable refined plate theories", *Adv. Nano Res.*, **18**(1), 187-212. https://doi.org/10.12989/anr.2024.18.1.187.

Bellifa, H., Halim Benrahou, K., Anis Bousahla, A., Tounsi, A. and Hassan, S. (2017), "A nonlocal zeroth-order shear deformation theory for nonlinear postbuckling of nanobeams", *Struct. Eng. Mech.*, **62**(6), 695-702, https://doi.org/10.12989/sem.2017.62.6.695.

Bessaim, A., Houari, M.S.A. and Tounsi, A. (2013), "A new higher-order shear and normal deformation theory for the static and free vibration analysis of sandwich plates with functionally graded isotropic face sheets", *J. Sandw. Struct. Mater.*, **15**(6), 671-703. https://doi.org/10.1177/1099636213510539.

Guo, H., Li, Y., Zhao, B., Guo, Y., Xie, Z., Morina, A. and Lu, X. (2024), "Transient lubrication of floating bush coupled with dynamics and kinematics of cam-roller in fuel supply mechanism of diesel engine", *Phys. Fluids*, **36**(12), 123103. https://doi.org/10.1063/5.0232226.

Guo, Y. and Alam, M. (2025), "Nonlinear bending and thermal postbuckling of magneto-electro-elastic nonlocal strain-gradient beam including surface effects", *Appl. Math. Model.*, **142**, 115955. doi: https://doi.org/10.1016/j.apm.2025.115955

Hu, H., Qi, L. and Chao, X. (2024), "Physics-informed Neural Networks (PINN) for computational solid mechanics: Numerical frameworks and applications", *Thin-Wall. Struct.*, **205**, 112495. doi: https://doi.org/10.1016/j.tws.2024.112495

Jain, N. and Kanu, N.J. (2021), "The potential application of carbon nanotubes in water treatment: A state-of-the-art review," *Mater. Today Proc.*, **43**, 2998-3005. https://doi.org/10.1016/j.matpr.2021.01.331.

Kanu, N.J., Gupta, E., Vates, U.K. and Singh, G.K. (2019a), "An insight into biomimetic 4D printing", *RSC Adv.*, **9**, 38209-38226. https://doi.org/10.1039/C9RA07342F.

Kanu, N.J., Gupta, E., Vates, U.K., Singh, G.K. (2019b), "Self-healing composites: A state-of-the-art review," *Compos. Part A Appl. Sci. Manuf.*, **121**, 474-486. https://doi.org/10.1016/j.compositesa.2019.04.012.

Kanu, N.J., Vates, U.K., Singh, G.K. and Chavan, S. (2019c), "Fracture problems, vibration, buckling, and bending analyses of functionally graded materials: A state-of-the-art review including smart FGMs", *Part. Sci. Technol.*, **37**, 583-608. https://doi.org/10.1080/02726351.2017.1410265.

Kanu, N.J., Patwardhan, D., Gupta, E., Vates, U.K. and Singh, G.K. (2020a), "Numerical investigations of stress-deformation responses in fractured paediatric bones with prosthetic bone plates," *IOP Conf. Ser. Mater. Sci. Eng.*, **814**, 012038. https://doi.org/10.1088/1757-899X/814/1/012038.

Lal, A. and Kanu, N.J. (2020b), "The nonlinear deflection response of CNT/nanoclay reinforced polymer hybrid composite plate under different loading conditions", *IOP Conf. Ser. Mater. Sci. Eng.*, **814**, 012033. https://doi.org/10.1088/1757-899X/814/1/012033.

Kanu, N.J., Gupta, E., Vates, U.K. and Singh, G.K. (2021a), "An insight into smart self-lubricating composites", *Smart Polym. Nanocompos. Biomed. Environ. Appl.*, **85-101**. https://doi.org/10.1016/B978-0-12-819961-9.00012-8.

Kanu, N.J., Patwardhan, D., Gupta, E., Vates, U.K. and Singh, G.K. (2021b), "Finite element analysis of mechanical response of fracture fixation functionally graded bone plate at paediatric femur bone fracture site under compressive and torsional loadings", *Mater. Today Proc.*, **38**, 2817-2823. https://doi.org/10.1016/j.matpr.2020.08.740.

Kanu, N.J., Patil, S.A., Sutar, V., Gupta, E., Singh, G.K., Vates, U.K. and Chavan, S. (2021c), "Design and CFD analyses of aluminium alloy-based vortex tubes with multiple inlet nozzles for their optimum performances in sustainable applications", *Mater. Today Proc.*, **47**, 2808-2813. https://doi.org/10.1016/j.matpr.2021.03.482.

Kanu, N.J., Mangalam, A., Gupta, E., Vates, U.K., Singh, G.K. and Sinha, D.K. (2021d), "Investigation on secondary deformation of ultrafine SiC particles reinforced LM25 metal matrix composites", *Mater. Today Proc.*, **47**, 3054-3058. https://doi.org/10.1016/j.matpr.2021.05.640.

Kanu, N.J. (2021e), "Modeling of stress wave propagation in matrix cracked laminates", *AIP Adv.*, **11**, 085217. https://doi.org/10.1063/5.0057749.

Gonfa, B.K., Sinha, D., Vates, U.K., Badruddin, I.A., Hussien, M., Kamangar, S., Singh, G.K., Ahmed, G.M.S., Kanu, N.J. and Hossain, N. (2022a), "Investigation of mechanical and tribological behaviors of aluminum-based hybrid metal matrix composite and multi-objective optimization", *Mater.*, **15**, 5607. https://doi.org/10.3390/ma15165607.

Kanu, N.J. and Lal, A. (2022b), "Post buckling responses of carbon nanotubes' fiber reinforced and nanoclay modified polymer matrix hybrid composite plate under in-plane buckling load using the higher order shear deformation theory", *Mech. Based Des. Struct. Mach.*, https://doi.org/10.1080/15397734.2022.2126985.

Liu, Y., Su, J., He, D., Hao, P., Liu, Y., Wang, Z. and Wang, T. (2025), "Analytical model for corrugated rolling of composite plates considering the shear effect", *J. Manuf. Process*., **134**, 1069-1081. https://doi.org/10.1016/j.jmapro.2025.01.025.

Özkılıç, Y.O., Aksoylu, C. and Arslan M.H. (2021) "Numerical evaluation of effects of shear span, stirrup spacing and angle of stirrup on reinforced concrete beam behaviour", *Struct. Eng. Mech.*, **79**(3), 309-326. https://doi.org/10.12989/sem.2021.79.3.309.

Pandey, V., Kanu, N.J., Singh, G.K. and Gadissa, B. (2021), "AZ31-alloy, H13-die combination heat transfer characteristics by using inverse heat conduction algorithm", *Mater. Today Proc.*, **44**, 4762-4766. https://doi.org/10.1016/j.matpr.2020.11.258.

Peng, X., Chen, K., Jia, W., Li, K., Huang, C. and Liu, X. (2025), "Stacking sequence optimization of variable thickness composite laminated plate based on multi-peak stacking sequence table", *Compos. Struct*., **356**, 118886. https://doi.org/10.1016/j.compstruct.2025.118886.

Reddy, J.N. and Wang, J. (2020), "A higher-order theory for the analysis of functionally graded plates with integrated piezoelectric layers", *J. Appl. Mech.*, **87**(2), 024501, https://doi.org/10.1115/1.4044570.

Singh, S. and Prakash, C. (2018), "Nonlinear static and dynamic analysis of functionally graded plates with thermal and mechanical loading", *J. Sandw. Struct. Mater.*, **20**(3), 367-392. https://doi.org/10.1177/1099636217741611.

Vates, U.K., Kanu, N.J., Gupta, E., Singh, G.K., Daniel, N.A. and Sharma, B.P. (2021), "Optimization of FDM 3D printing process parameters on ABS based bone hammer using RSM technique", *IOP Conf. Ser. Mater. Sci. Eng.*, **1206**, 012001. https://doi.org/10.1088/1757-899X/1206/1/012001.

Wang, G., Sun, L. and Zhang, C. (2024a), "The effect of polyvinylpyrrolidone modified nano-polymers on rheological properties of silicon-based shear thickening fluid", *Phys. Fluids*, **36**(7), 073108. https://doi.org/10.1063/5.0213620.

Wang, Z., Yuan, Y., Zhang, S., Lin, Y. and Tan, J. (2024b), "A multi-state fusion informer integrating transfer learning for metal tube bending early wrinkling prediction", *Appl. Soft Comput.*, **151**, 110991. https://doi.org/10.1016/j.asoc.2023.110991.

Wang, Z., Li, J., Yuan, Y., Zhang, S., Hu, W., Ma, J., and Tan, J. (2025), "Digital-twin-enabled online wrinkling monitoring of metal tube bending manufacturing: A multi-fidelity approach using forward-convolution-GAN", *Appl. Soft Comput*., **171**, 112684. doi: https://doi.org/10.1016/j.asoc.2024.112684

Yao, S., Chen, Y., Sun, C., Zhao, N., Wang, Z. and Zhang, D. (2024), "Dynamic response mechanism of thin-walled plate under confined and unconfined Blast Loads", *J. Mar. Sci. Eng*., **12**(2), 224. doi: https://doi.org/10.3390/jmse12020224

Zhao, Y., Lu, Z., Gedela, R., Tang, C., Feng, Y., Liu, J. and Yao, H. (2025a), "Performance and geocell-soil interaction of sand subgrade reinforced with high-density polyethylene, polyester, and polymer-blend geocells: 3D numerical studies", *Comput. Geotech*., **178**, 106949. https://doi.org/10.1016/j.compgeo.2024.106949.

Zhao, Y., Xiao, H., Chen, L., Chen, P., Lu, Z., Tang, C. and Yao, H. (2025b), "Application of the non-linear three-component model for simulating accelerated creep behavior of polymer-alloy geocell sheets", *Geotext. Geomembranes*., **53**(1), 70-80. doi: https://doi.org/10.1016/j.geotexmem.2024.09.005

Zhou, L., Riska, K. and Ji, C. (2017), "Simulating transverse icebreaking process considering both crushing and bending failures", *Marine Struct*., **54**, 167-187. https://doi.org/10.1016/j.marstruc.2017.04.004.

Zhou, L., Gao, J., Xu, S. and Bai, X. (2018), "A numerical method to simulate ice drift reversal for moored ships in level ice", *Cold Reg. Sci. Technol*., **152**, 35-47. https://doi.org/10.1016/j.coldregions.2018.04.008.

CC